EXPERIMENTAL INVESTIGATION OF FRICTION BASED ON ULTRASONIC VIBRATION

Changli ZHA[1], Shenlong ZHA [2]

The effects of punch radius, deep-drawing speed and amplitude on the friction coefficient were studied on an improved drawing-bulging friction coefficient measurement platform on basis of ultrasonic vibration. The changes of friction coefficient curves were more gentle at larger deep-drawing speed, and the friction coefficient declined as the vibration amplitude increases. From no ultrasonic vibration to the amplitude of 10.1 μm, the friction coefficients at the punch radii R0.3 and R1.5 declined from 0.18 to 0.13 and from 0.12 to 0.11 respectively. The friction coefficients of thin specimens were larger than thick specimens whether ultrasonic vibration was applied or not.

Keywords: Ultrasonic vibration; Friction coefficient; Surface effect; Drawing-bulging

1. Introduction

Ultrasonic vibration-assisted metal plastic forming can effectively decrease forming force and contact friction and improve surface quality of formed parts. Thus, this process, especially microplastic metal material forming, is extensively applied into stamping [1-4], brushing [5], upsetting [6-7], spinning [8], cutting and other technical fields [9-11].

Since microplastic metal forming is different from metal macro-forming, friction directly affects the forming properties and quality of formed metal parts. Hence, the friction during micro-forming processes has been a research hotspot. Experimentally, Siegert et al. applied ultrasonic vibration into a strip-drawing process to study the effects on friction and found the decrease of frictional force and the improvement of surface quality were both associated with the vibration amplitude and deep-drawing speed [12]. Ngaile and Bunget probed into extrusion micro-forming of aluminium materials and copper materials and noticed that the surface quality of formed parts was obviously improved under ultrasonic vibration [13]. During micro-upsetting experiments, ultrasound significantly affected surface roughness parameter Ra, which considerably dropped from 1.376μm to

[1] Prof., Electronic Engineering and Intelligent Manufacturing, Anqing Normal University, China, e-mail: zhachangli@126.com
[2] PhD, Electronic Engineering and Intelligent Manufacturing, Anqing Normal University, China, e-mail: zslwinner@163.com

0.77μm after the application of ultrasonic vibration [14]. Hung et al. determined friction calibration curves and friction factors through the finite element method through upsetting experiments on the ring compression of aluminum alloys, and further quantitatively analyzed the relation between friction coefficient and ultrasonic vibration through double-cup extrusion experiments, which showed ultrasonic vibration significantly affected the friction factor [15]. Moreover, at the theoretical level, the existing research is focused on in-plane and out-of-plane aspects. Tsai et al. proposed a theoretical method based on the Dahl friction model and found friction was lowered when tangential vibration occurred at any in-plane angle [16]. Popov et al. elaborated the effects of large-amplitude in-plane frictional contact on hardness [17-20]. Teidelt et al. theoretically studied the effects of out-of-plane normal ultrasonic vibration on static friction and slide friction [21-22]. Based on a simplified model, Popov et al. constructed a friction reduction theoretical model of out-of-plane applied ultrasound against velocity vibration amplitude and displacement amplitude [17]. The above studies empirically underlie the qualitative interpretation and analysis concerning the effects of ultrasonic vibration on contact friction, but the results of theoretical models and experiments are inconsistent to some extent.

For this reason, a frictional property test installation about SUS304 sheets under ultrasonic vibration was designed and used to simulate the friction status during practical deep drawing forming. The friction coefficients of specimens with different thicknesses, mould dimensions, deep-drawing speeds and amplitudes during deep-drawing forming were studied. The effects of thickness, mould, deep-drawing speed and amplitude on friction coefficient were analyzed.

2. Experimental

Metal sheet drawing-bulging experiments under ultrasonic vibration for friction coefficient measurement were conducted to investigate the effects of specimen sizes, deep-drawing speed and punch radius on contact friction force, or namely the variation of friction coefficient. In practice, however, the friction coefficient of metal plastic forming is affected by many factors, including stamping velocity, mould dimension parameters, lubrication status, and temperature. To display the actual metal plastic forming as much as possible, we modified the traditional drawing-bulging friction coefficient measurement method and built a metal sheet drawing-bulging friction coefficient measurement platform based on ultrasonic vibration and used it to evaluate contact friction. During drawing-bulging experiments, a metal sheet passed two cylindrical friction heads fixed below the lower mould, and the two ends of the sheet were fixed on the upper mould. The punch mould formed from deep drawing was simulated through the two cylindrical friction heads, and the diameters of the friction heads were

changed to alter the punch radius. Under external loading, the upper mould moved upwards, so the middle segment and the straight wall segment on the metal sheet generated different strains, and then the tensile forces at the two segments were calculated separately. Finally, the average friction coefficient on the contact surface was computed. In actual deep-drawing forming, however, deep drawing and bending occur simultaneously. Hence, Wang et al. modified the drawing-bulging measuring method by adding the contact between cylindrical friction heads and metal specimens and simulated the co-occurrence of deep drawing and bending through a progressive contact form or namely with the contact angle gradually rising from zero. Our experiment platform was based on the modified method of Wang et al. [23], but we replaced the cylindrical friction heads with punch molds with varying punch radius. The deep-drawing forming was realized by the downward movement of punch molds. The working principle was illustrated in Fig. 1.

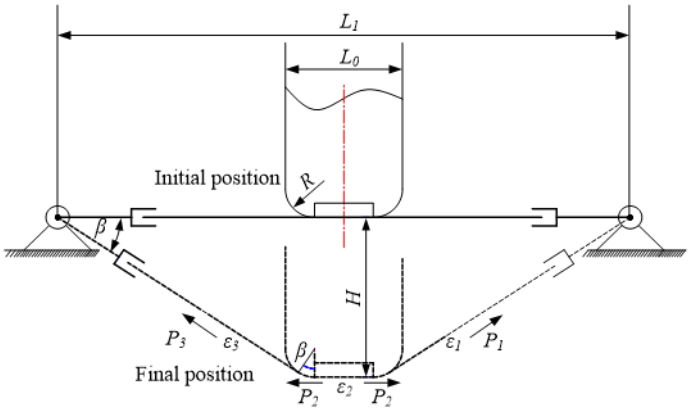

Fig. 1. Schematic illustration of the friction coefficient testing device

The metal sheet drawing-bulging friction coefficient measurement platform based on ultrasonic vibration is illustrated in Fig. 2. This platform consists of a CMT4203 electronic universal tensile testing machine, an ultrasonic generator, an energy converter, amplitude transformers, clamping parts, force sensors, digital display, and upper indenters (punch molds).

To simulate the effects of punch radius on friction during actual deep drawing forming, we designed upper indenters (punch molds) with varying sizes in a modularized way for friction coefficient measurement. To avoid the interference of contact between specimens and mould lower surfaces, we concaved the lower surfaces of punch molds. In the meantime, to avoid the interference from the substances attached to the punch molds and from the impurities inside the punch molds, we precisely ground and polished the punch molds. The real object of a punch mould is shown in Fig. 3.

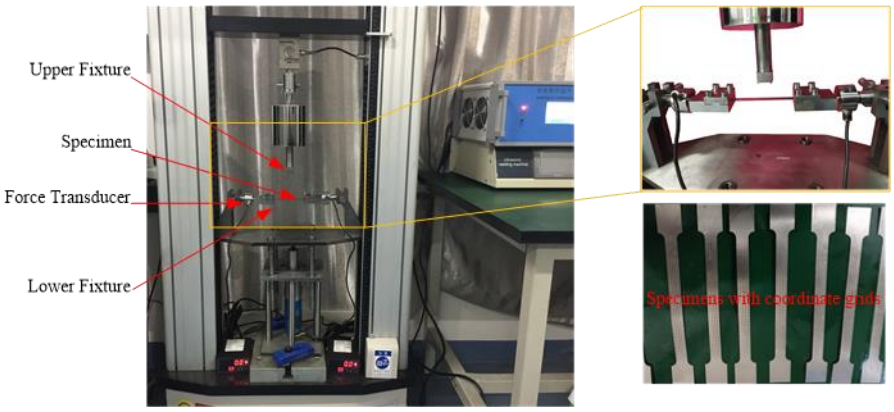

Fig. 2. Friction coefficient testing device

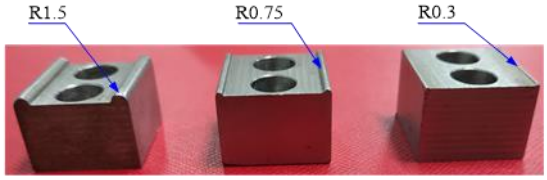

Fig. 3 . Upper pressure head (punch)

The effects of deep-drawing speed, specimen thickness and amplitude on the friction coefficient were studied. The concrete working parameters were listed in Table 1. The rated excited frequency of the ultrasonic generator was 19.891 Khz, and its peak power output was 2 kW. The specimens were polished, cleaned, and made into surface printed grids by an electrochemical corrosion method. The grid dots were in diameter of 1 mm and distance of 2 mm. The long axis and short axis strains of each grid dot after deformation were measured using an electron microscope. The specimen working sizes and the real object after gridding were shown in Fig. 4. During the experiments, each specimen was repeated at least 3 times under each scheme, which ensured the effectiveness of the experimental results.

Table 1

Experimental parameters of friction coefficient measurement

Parameters	value
Drawing speed（mm/s）	0.1
	10
thickness（mm）	0.1
	0.2
Vibration amplitude（μm）	3.9
	7.8
	10.1

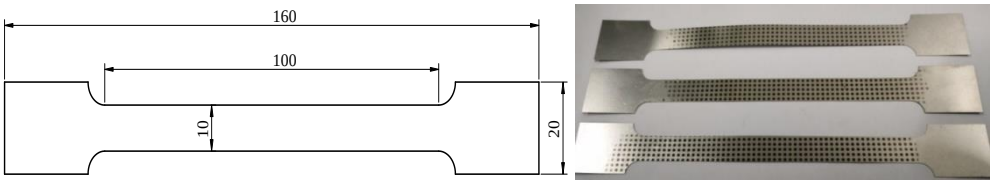

(a) (b)

Fig. 4. The shape and size of SUS304 specimen/mm (a)the size of specimen/mm, (b) specimen with printed grid

According to the friction coefficient measurement principle (Fig. 1), the pulling forces P_1 and P_3 at the left and right straight parts of each specimen were measured using a force sensor, and the measured data were fed back to digital display. Then P_1=P_3 was adjusted according to structure principle and force balance. The pull P_2 at the middle of each specimen was determined indirectly: the long axis and short axis strains of each printed grid dot after deformation were measured firstly, then the corresponding stress was determined according to the tensile stress strain curve of SUS304 [24] and finally, P_2 was calculated according to a function.

Hence, P_2 can be computed as follows:

$$P_2 = \sigma_1 wt \tag{1}$$

where σ_1 is the instant principal stress, w is specimen width, and t is specimen thickness. At this time, the friction coefficient was calculated as follows [25]:

$$\mu_e = \frac{1}{\beta} \ln \frac{P_1}{P_2} \tag{2}$$

where β is the contact wrap angle between a specimen and a punch mould and it varies with the change of punch mould stroke and meets the following equation:

$$A\sin\beta + B\cos\beta = 1 \tag{3}$$

At $0 \le \beta \le \frac{\pi}{2}$, we have $A = \frac{L_1 - L_0 + 2R}{2R}$ and $B = \frac{R - H}{R}$ Then β can be determined according to the punch mould stroke H.

The friction coefficients at varying punch radius (R0.3/ R0.75/ R1.5) and at the experimental parameters in Table 1 were measured, and the effects of each parameter on the friction coefficients were analyzed.

3. Results and Discussion

When the punch radius was R0.3 and thickness was 0.1 mm, the friction coefficients at low and high deep drawing speeds (0.1, 10 mm/s) were measured (Fig. 5).

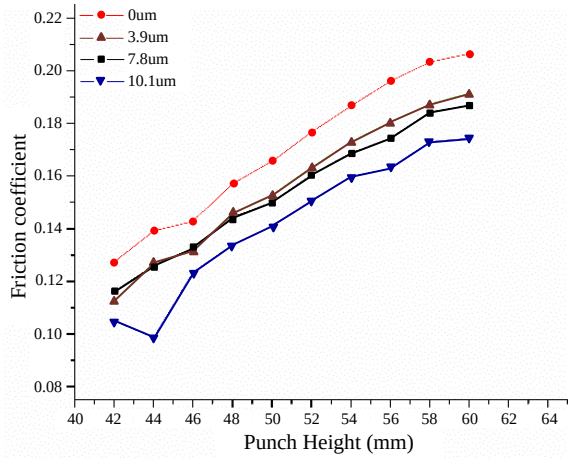

(a)

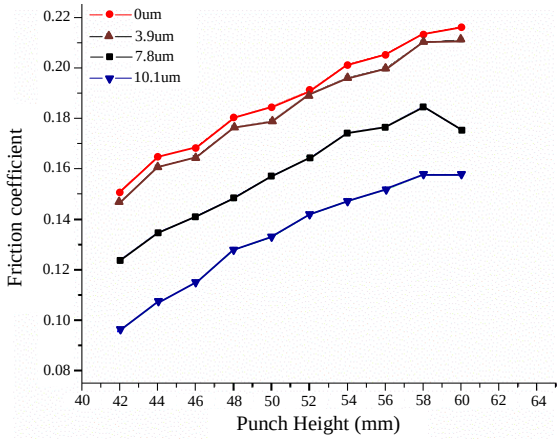

(b)

Fig. 5. Friction coefficient under different drawing speed (a) drawing speed 0.1mm/s, (b) drawing speed 10mm/s

The applied ultrasonic vibration significantly affected the friction coefficients under both deep drawing speeds (0.1 and 10 mm/s) (Fig. 5). The change of friction coefficient curve in Fig. 5(b) is gentler than that in Fig. 5(a). This was mainly because (1) the increased drawing speed led to a shorter contact time between punch molds and specimens, which lowered the various accumulative effects on the contact surface, and (2) the smaller molecular

attraction between contact surfaces resulted in a smaller friction coefficient. As the ultrasonic vibration amplitude rose, the friction coefficient decreased, and the decreased value at low velocity was approximately uniformly distributed, but at high drawing velocity, the effects of vibration amplitudes on the decreased values of friction coefficient were largely different. At the same drawing height, the friction coefficients at the amplitudes of 7.8 and 10.1 μm at drawing velocity of 0.1 and 10 mm/s decreased by 6.7% and 18.8% respectively.

The punch radius affected the friction and bending deformation during drawing forming to some extent. Hence, the effects of 3 punch radii (R0.3, R0.75, R1.5) on the friction coefficient were studied.

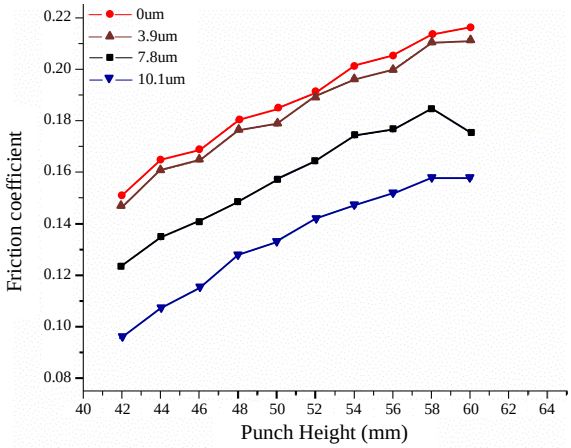

(a)R0.3

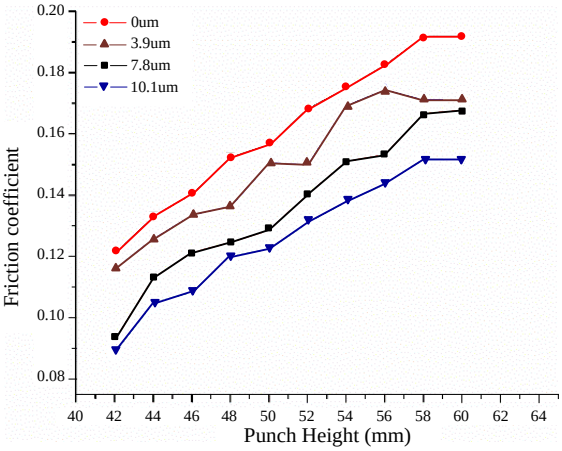

(b)R0.75

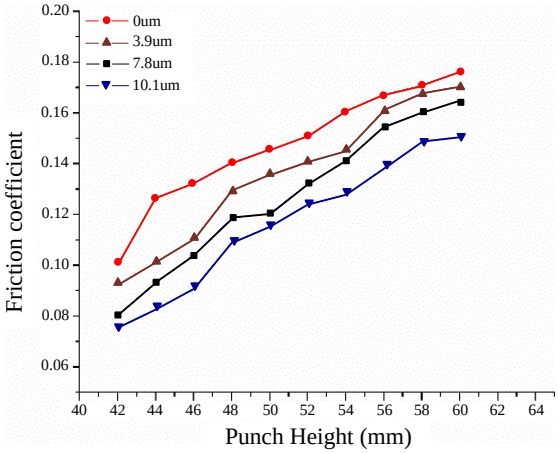

(c)R1.5

Fig. 6**.** Friction coefficient under different punch fillet radius (a) R0.3, (b) R0.75, and (c) R1.5

Clearly, the punch radius significantly affected the friction coefficient (Fig. 6). As the punch radius rose, the friction coefficient declined. Without the ultrasonic vibration, the friction coefficients at drawing height of 50 mm corresponding to R0.3 and R1.5 were 0.18 and 0.12 respectively. With the vibration at amplitude of 10.1 μm, the friction coefficients became 0.13 and 0.11 respectively, indicating the applied ultrasonic vibration more sensitively affected the smaller punch radius.

During practical drawing forming, the bending deformation differs along with the sheet thickness. The differences in thickness induce additional pull forces to the middle and straight- wall parts of sheets, thereby affecting the friction coefficient. When the pull force caused by bending deformation during deep drawing is considered, the friction coefficient can be expressed as [23]:

$$\mu_e' = \frac{1}{\beta} \ln \frac{P_1 - \Delta P}{P_2 + \Delta P} \tag{4}$$

where ΔP is the additional pulling force induced by bending deformation.

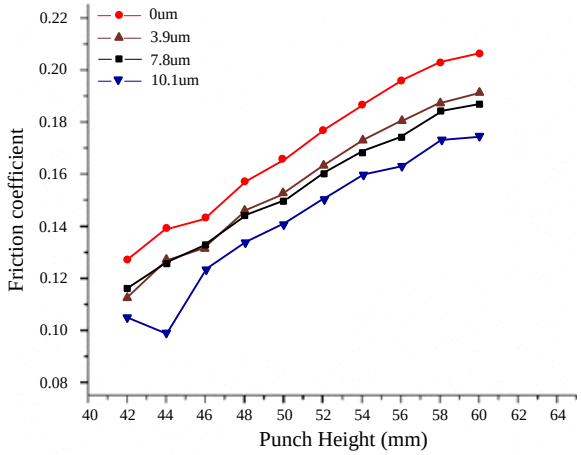

(a)

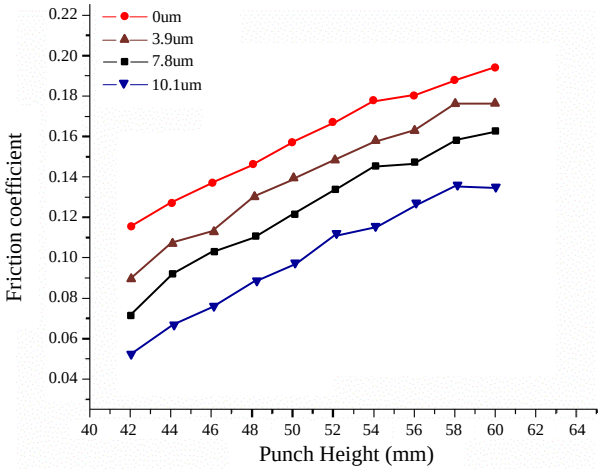

(b)

Fig. 7. Friction coefficient under different thickness (a) thickness 0.1mm, and (a) thickness 0.2mm

At the drawing speed of 0.1 mm/s and punch radius R0.3, the friction coefficients at the thickness of 0.2 mm were always smaller compared with the thickness of 0.1 mm, whether ultrasonic vibration was applied or not (Fig. 7). Thinner specimens were more prone to bending deformation and at this time, the additional pulling forces at the middle part and at both sides of straight walls were small. According to Eq. (4), the resulting friction coefficients were larger than at the thickness of 0.2 mm, so the experimental results are consistent with theoretical results.

4. Conclusions

The effects of punch radius, deep-drawing speed and amplitude on the friction coefficient were studied on a friction coefficient measurement platform assisted by ultrasonic vibration. A contact friction model based on the tribology theory of adhesion and plowing was constructed and used to explain the antifriction surface effects of applied out-of-plane normal vibration. Together with experimental results, relevant parameters of the theoretical model were calibrated and used to analyze modeling precision.

1. The deep-drawing speed significantly affected the friction coefficient, and the friction coefficient curve at a larger speed changed more gently when other experimental parameters were the same. As the ultrasonic vibration amplitude rose, the friction coefficient decreased, and the decreased value at low drawing speed was almost uniformly distributed, but at high drawing speed, the effects of vibration amplitudes on the decreased values of friction coefficient were largely different. At the same drawing height, the friction coefficients at the amplitudes of 7.8 and 10.1 μm at drawing speed of 0.1 and 10 mm/s decreased by 6.7% and 18.8% respectively.

2. With the absence of ultrasonic vibration, the friction coefficients at drawing height of 50 mm corresponding to R0.3 and R1.5 were 0.18 and 0.12 respectively. After the vibration at amplitude of 10.1 μm was applied, the friction coefficients became 0.13 and 0.11 respectively, indicating the effect of the applied ultrasonic vibration was more sensitive at the smaller punch radius.

3. When other experimental parameters were the same, since thinner specimens were more prone to bending deformation, the additional pulling forces at the middle and at two sides of straight walls were small and consequently, the friction coefficients of thinner specimens surpassed those of thicker specimens whether ultrasonic vibration was applied or not.

Acknowledgement

This work was financially supported by the Natural Science Foundation of Educational Commission of Anhui Province of China (Grant No. KJ2019A0576).

R E F E R E N C E S

[1]. *Han G , Li K , Peng Z* , et al. A new porous block sonotrode for ultrasonic assisted micro plastic forming[J]. The International Journal of Advanced Manufacturing Technology, 94(5-8)p.1-10, 2016.

[2]. *Zhe Li, DaoguoYang, Weidong Hao, et al*. A novel technique for micro-hole forming on skull with the assistance of ultrasonic vibration[J]. Journal of the Mechanical Behavior of Biomedical Materials, 57, p.1-13,2016.

[3]. *Kriechenbauer, Sebastian, Mauermann, Reinhard, Muller, Peter.* Deep Drawing with Superimposed Low-frequency Vibrations on Servo-screw Presses[J]. Procedia Engineering, 81, p.905-913, 2014.
[4]. *Seo Y H , Park C J , Kim B H , et al*. Development of audio frequency vibration microforming system[J]. International Journal of Precision Engineering and Manufacturing, 13(5), p.789-794, 2012.
[5]. *Liu S, Shan X, Guo K, et al.* Experimental study on titanium wire drawing with ultrasonic vibration[J]. Ultrasonics, 83, p. 60-67,2018.
[6]. *Behrens G , Trier F O , Tetzel H , et al*. Influence of tool geometry variations on the limiting drawing ratio in micro deep drawing[J]. International Journal of Material Forming,9(2), p.253-258,2016.
[7]. *Yanxiong, Liu, Sergey, et al*. Comparison Between Ultrasonic Vibration-Assisted Upsetting and Conventional Upsetting[J]. Metallurgical&Materials Transactions A,3232(44A),p.1-13,2013.
[8]. *Rasoli M A , Abdullah A , Farzin M , et al*. Influence of ultrasonic vibrations on tube spinning process[J]. Journal of Materials Processing Technology, 212(6),p.1443-1452,2012.
[9]. *Tan R, Zhao X, Guo S, et al*. Sustainable production of dry-ultra-precision machining of Ti–6Al–4V alloy using PCD tool under ultrasonic elliptical vibration-assisted cutting[J]. Journal of Cleaner Production, 248, p.1-44,2020.
[10]. *Zhu L, Ni C, Yang Z, et al*. Investigations of micro-textured surface generation mechanism and tribological properties in ultrasonic vibration-assisted milling of Ti–6Al–4V[J]. Precision Engineering, 57, p.229-243,2019.
[11]. *Gunduz I E , Mcclain M , Cattani P , et al.* 3D printing of extremely viscous materials using ultrasonic vibrations[J]. Additive Manufacturing, 22, p.98-103,2018.
[12]. *Siegert K , Ulmer J* . Influencing the Friction in Metal Forming Processes by Superimposing Ultrasonic Waves[J]. CIRP Annals - Manufacturing Technology,50(1), p.195-200, 2001.
[13].*Bunget C , Ngaile G* . Influence of ultrasonic vibration on micro-extrusion[J]. Ultrasonics, 51(5),p.606-616, 2011.
[14]. *Yao Z , Kim G Y , Faidley L A , et al*. Effects of superimposed high-frequency vibration on deformation of aluminum in micro/meso-scale upsetting[J]. Journal of Materials Processing Technology,212(3), p.640-646,2012.
[15]. *Hung J C , Huang C C* . Evaluation of friction in ultrasonic vibration-assisted press forging using double cup extrusion tests[J]. International Journal of Precision Engineering and Manufacturing, 13(12),p. 2103-2108, 2012.
[16]. *C. C. Tsai · C. H. Tseng*. The effect of friction reduction in the presence of in-plane vibrations[J]. Archive of Applied Mechanics, 75(2-3),p.164-176, 2006.
[17]. *Popov M , Popov V L , Popov N V* . Reduction of friction by normal oscillations. I. Influence of contact stiffness[J]. Friction, 2017, 5(1):45-55.
[18]. *Mao X , Popov V L , Starcevic J , et al*. Reduction of friction by normal oscillations. II. In-plane system dynamics[J]. Friction, 5(2),p.194-206,2017.
[19]. *Popov M.* Critical velocity of controllability of sliding friction by normal oscillations in viscoelastic contacts[J]. Mechanical Engineering ,14(3),p. 335–341,2016.
[20]. *Popov V L , Pohrt R , Hess M* . General procedure for solution of contact problems under dynamic normal and tangential loading based on the known solution of normal contact problem[J]. The Journal of Strain Analysis for Engineering Design, 51(4),p.1-9,2016.
[21]. *Teidelt E , Willert E , Filippov A E , et al.* Modeling of the dynamic contact in stick-slip microdrives using the method of reduction of dimensionality[J]. Physical Mesomechanics, 15(5-6), p.287-292, 2012.

[22] *Teidelt E , Starcevic J , Popov V L* . Influence of Ultrasonic Oscillation on Static and Sliding Friction[J]. Tribology Letters, 48(1),p.51-62, 2012.
[23]. *Wang W , Wagoner R H , Wang X J* . Measurement of friction under sheet forming conditions[J]. Metallurgical and Materials Transactions A, 27(12), p.3971-3981,1996.
[24]. *Zha C L , Chen W* . Theories and experiments on effects of acoustic energy field in micro-square cup drawing[J]. The International Journal of Advanced Manufacturing Technology, 104(9-12),p.4791-4802, 2019.
[25]. *Archie Higdon , William B. Stiles*. Engineering mechanics[J]. New York, Prentice-Hall, Inc., 249(4), p.0-505, 1949.